coatings

MDPI

Review

Cellulose Aerogels for Thermal Insulation in Buildings: Trends and Challenges

Danny Illera *, Jaime Mesa, Humberto Gomez and Heriberto Maury

Department of Mechanical Engineering, Universidad del Norte, Barranquilla 081007, Colombia; jamesa@uninorte.edu.co (J.M.); humgomez@uninorte.edu.co (H.G.); hmaury@uninorte.edu.co (H.M.)
* Correspondence: dillera@uninorte.edu.co; Tel.: +57-5-350-9272

Received: 17 August 2018; Accepted: 27 September 2018; Published: 28 September 2018

Abstract: Cellulose-based aerogels hold the potential to become a cost-effective bio-based solution for thermal insulation in buildings. Low thermal conductivities (<0.025 $W \cdot m^{-1} \cdot K^{-1}$) are achieved through a decrease in gaseous phase contribution, exploiting the Knudsen effect. However, several challenges need to be overcome: production energy demand and cost, moisture sensitivity, flammability, and thermal stability. Herein, a description and discussion of current trends and challenges in cellulose aerogel research for thermal insulation are presented, gathered from studies reported within the last five years. The text is divided into three main sections: (i) an overview of thermal performance of cellulose aerogels, (ii) an identification of challenges and possible solutions for cellulose aerogel thermal insulation, and (iii) a brief description of cellulose/silica aerogels.

Keywords: cellulose; aerogel; thermal insulation; building envelope; silica

1. Introduction

Indoor space heating/cooling accounts for over 30% of all the energy consumed in buildings and around 10% of the world's energy consumption [1]. The building envelope thermal performance is a prime factor dictating the amount of energy required for environmental comfort. The building envelope is composed of different elements such as walls and roofs, which separate indoor and outdoor spaces. In this regard, several studies conclude an improvement in energy consumption by the incorporation of thermal insulation materials in walls and roofs as a passive strategy. For example, reductions in annual cooling energy and peak cooling load of up to 20% and 30% were achieved for a building located in a tropical region via implementation of the aforementioned strategy [2]. A thermal insulation material could be defined as one that slows down the heat flow into or out of the building. For its selection, thermal conductivity is the main property to look for. Table 1 lists the typical thermal conductivities of selected commercial building insulation materials for reference. These commercial materials are either derived from petrochemical sources or demand energy-intensive production processes, imparting questions about their role in a future sustainable economy, thus motivating the development of a family of renewable insulation materials and their corresponding low-energy demand processes [3].

Table 1. Thermal conductivity of selected building insulation materials [4].

Material	Thermal Conductivity ($W \cdot m^{-1} \cdot K^{-1}$)
Expanded polystyrene	0.030–0.040
Polyurethane	0.020–0.030
Fiberglass	0.033–0.044
Mineral wool	0.030–0.040

Cellulose is the most abundant bio-polymer on earth, recognized for its renewability, bio-compatibility, and bio-degradability. Cellulose is a linear polysaccharide (β (1−4) linked D-glucose units) generally found as a structural component of cell walls in plants and algae or as a biofilm secretion of some bacteria species. Secondary interactions (van der Waals and hydrogen bonding) between polymer chains promote parallel stacking and subsequent formation of fibrils with a diameter around 5–50 nm containing crystalline and amorphous regions [5]. These fibrils have a density around 1.5 $g \cdot cm^{-3}$, an average Young modulus of 125 GPa, an average tensile strength of 2.5 GPa, and a surface area close to 800 $m^2 \cdot g^{-1}$. Therefore, cellulose nanofibrils are suitable for the formation of bio-based aerogels for thermal insulation [6].

According to the International Union of Pure and Applied Chemistry (IUPAC), an aerogel refers to a gel comprising a microporous solid in which the dispersed phase is a gas [7]. An aerogel comprises a solid-smoke look alike and highly porous solid (porosity >90% typically). The bulk density of aerogels typically lies between 0.003–0.200 $g \cdot cm^{-3}$ and the surface area between 800–1000 $m^2 \cdot g^{-1}$ [8]. A distinction must be made between foams and aerogels. According to Sakai et al. [9], foams tend to have microscale pores with a wall-like solid phase, whereas aerogels have nanoscale pores formed with a network-like skeleton of interconnected nanoparticles (refer to Figure 1).

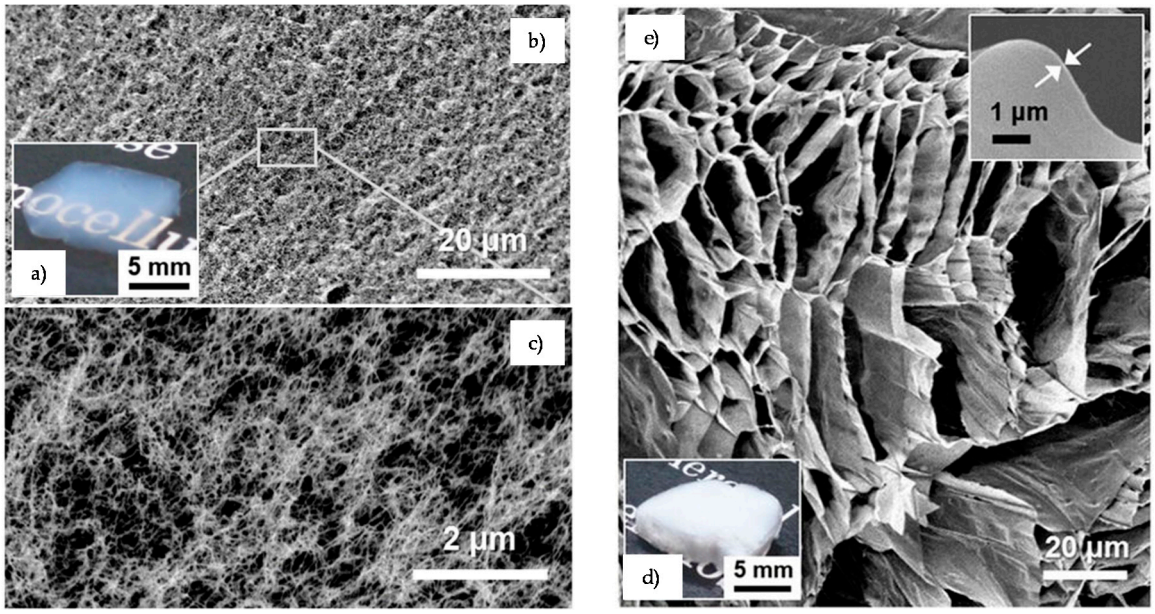

Figure 1. (**a**) Physical appearance of a cellulose aerogel; (**b**,**c**) Scanning electron microscopy images of a cellulose aerogel at different magnifications; (**d**) Physical appearance of a cellulose foam; (**e**) Scanning electron microscopy images of a cellulose foam. Reproduced from Sakai et al. [9], licensed under a Creative Commons Attribution 4.0 International License.

Cellulose aerogels are produced principally by a multistep sol−gel process involving dissolution of cellulose into nanofibrils, solvent exchange, and solvent removal by either supercritical-drying (SD) or freeze-drying (FD) [10–12]. The main technical challenge associated with this approach is to preserve the distribution of the dispersed solids upon solvent removal in order to get a porous material. During supercritical-drying, the solvent is substituted by a fluid at supercritical conditions (CO_2 is the common choice) to prevent the formation of a liquid/vapor interface, and thus, capillary pressure-induced stresses during removal that could lead to collapse of the porous structure. Freeze-drying involves rapid solidification of the dispersion typically by immersion in liquid nitrogen. The solidified solvent (water is the common choice) is then removed by sublimation to prevent the formation of a liquid/vapor interface (refer to Figure 2).

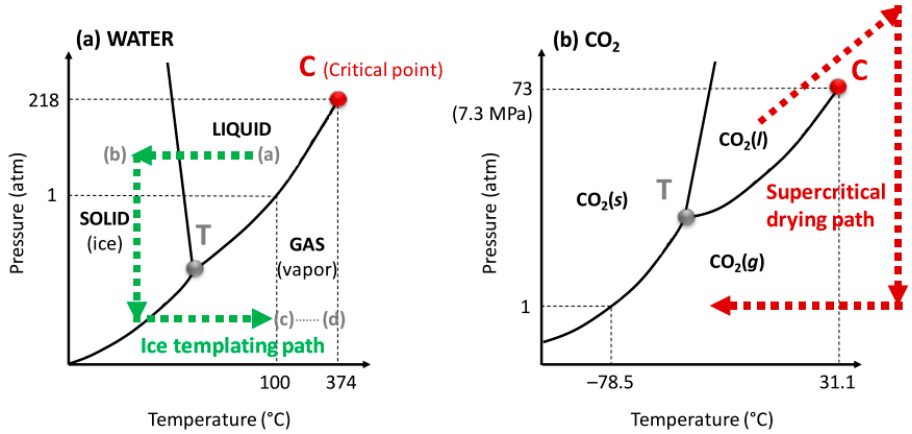

Figure 2. Phase diagrams of freeze-drying (**a**) and supercritical-drying (**b**) superposed on water and CO_2, respectively. Reproduced from from Lavoine & Bergström [10], licensed under a Creative Commons Attribution Non-Commercial 3.0 Unported License.

The thermal conductivity of a porous material like an aerogel could be divided into three contributions: conduction of the solid network, conduction of the gaseous phase, and radiation through or within pores [13]. The contribution of the solid network decreases as the porosity increases because a large quantity of pores restricts the propagation of phonons in the aerogel backbone [14]. The contribution of the gaseous phase is due to elastic collisions between gas molecules. The thermal conductivity of the gaseous phase depends on the mean free path of the gas molecules enclosed in the pores and the pore size. In principle, for the aerogel to be effective designed, its thermal conductivity should be lower than the thermal conductivity of "free" atmospheric air (0.025 $W \cdot m^{-1} \cdot K^{-1}$ at 300 K and 1 atm [15]). The aforementioned is achieved by the presence of pore sizes below the mean free path of air molecules (70 nm at 300 K and 1 atm), thus inhibiting the thermal diffusion of the gas (often call the Knudsen effect [16]). The ratio of the mean free path of gas molecules and the diameter of the pore is known as the Knudsen number. The nanometric size of the pores suppresses gaseous convective thermal transport and radiation.

2. Thermal Performance of Cellulose Aerogels

Cellulose nanofibrils, the building block of cellulose aerogels, present a natural variability as a function of the feedstock and extraction process. Chen et al. [17] measured the thermal properties of cellulose aerogels formed from fibrils extracted by four isolation methods: high-intensity ultra-sonication, hydrochloric acid hydrolysis, (2,2,6,6-tetramethylpiperidin-1-yl) oxidanyl (TEMPO)-mediated oxidation, and sulfuric acid hydrolysis. The highest thermal degradation temperature (342 °C) was reported for the case of hydrochloric-acid hydrolysis-mediated isolation. The lowest thermal degradation temperature (120 °C) corresponded to the case of sulfuric-acid hydrolysis-mediated isolation, attributed to the presence of sulfate groups on the fibril surface. All the aerogels reported thermal conductivities below 0.016 $W \cdot m^{-1} \cdot K^{-1}$ as a consequence of their low densities (0.005 $g \cdot cm^{-3}$) and high porosities.

Surface properties of cellulose nanofibrils also affect the aerogel formation process and final properties. For example, consistent gel formation with sulfated cellulose nanofibrils tends to be more difficult than with carboxylated cellulose nanofibrils [18]. Therefore, aiming to mimic the optical transparency and linear elasticity of silica aerogels, Kobayashi et al. [19] prepared aerogels from surface-carboxylated cellulose nanofibrils dispersed in water in a nematic liquid-crystal order. The lowest thermal conductivity reported was 0.018 $W \cdot m^{-1} \cdot K^{-1}$ for the case of an aerogel with a density of 0.017 $g \cdot cm^{-3}$ and a pore size of approximately 30 nm. The key for obtaining such properties was the preservation of the liquid-crystalline arrangements during the formation of the aerogels.

Regarding the role of morphology on the thermal performance of aerogels, Sakai et al. [9] compared cellulose foams and aerogels with a solid volume fraction ranging from 0.3% to 2.7% made of crystalline cellulose nanofibers. For the case of the foam, the thermal conductivity decreased as the solid volume fraction increased. In principle, the conductivity of air within a microscale pore is due to convection, and thus, has the same conductivity as atmospheric air. However, heat transfer between air and the solid phase plays a major role in the overall conductivity due to the non-interconnected arrangement of the porous structure. Therefore, the tendency between thermal conductivity and solid volume fraction is explained by an increase in the contribution of the interfacial heat transfer as the pore size decreases with the rise in solid volume fraction. For the case of the aerogels, the thermal conductivity increased as the solid volume fraction did. For this case, heat transfer between the gas and solid phases is negligible due to the presence of open pores. Jiménez-Saelices et al. [20] also evaluated the thermal properties of cellulose aerogels as a function of different pore organizations. The aerogels were formed from cellulose nanofibril suspensions by freeze-drying, using two different molds subjected to different temperature gradients. Two cases were evaluated: one aerogel with oriented pore channels and an aerogel with no pore alignment. At a fixed density, aerogels with no pore alignment had more efficient thermal insulating properties than aerogels prepared with oriented pore distribution, and attained a minimal thermal conductivity of 0.024 $W \cdot m^{-1} \cdot K^{-1}$. Although, for the former case, the pores are microscopic; the reduction in thermal conductivity was associated with a decrease in heat transfer by radiation due to the absence of interconnecting channels between pores. This effect is further evidenced in the difference between the thermal conductivity in the transverse (0.030 $W \cdot m^{-1} \cdot K^{-1}$) and axial directions (0.060 $W \cdot m^{-1} \cdot K^{-1}$) of hierarchal aligned cellulose nanofibril foams [21].

Bendahou et al. [22] obtained aerogels with a foam-like morphology; i.e., pores with a wall-like solid phase. The team used nanozeolites and cellulose fibrils to form composite aerogels, expecting a synergy between components. The thermal conductivity decreased 0.028 $W \cdot m^{-1} \cdot K^{-1}$ to 0.018 $W \cdot m^{-1} \cdot K^{-1}$ as the mass fraction of nanoparticles increased. The trend in thermal conductivity was associated with the co-existence of nanozeolite pores and interfibrillar cellulose pores. The porous zeolites were embedded in the mesoporous nanofibrillated structure, thus reducing the gas molecule movement as the mass fraction of the former increased. It is worth noting that the thermal conductivity is similar to the all-cellulose aerogels previously discussed. This behavior could be attributed to the fact that microscopy observation reveaeds that nanozeolites were deposited on cellulose nanofibril films and that the thermal conductivity was relatively high because of the solid conduction between nanofibril films.

Seantier et al. [23] formed aerogels based on combinations of cellulose fiber and cellulose nanofibrils aiming toward tuning the thermal and mechanical properties through aspect ratio and mass proportion modification. The structure of the aerogels could be described as nanofibril films coated upon cellulose fibers. The lowest thermal conductivity reported was 0.023 $W \cdot m^{-1} \cdot K^{-1}$. The insulation performance was described as an interplay between meso- and nanopores. The nanopores were more effective in confining air through the Knudsen effect.

Jiménez-Saelices et al. [24] claimed that the reason for limited reports of aerogels prepared through freeze-drying showing thermal conductivities below 0.020 $W \cdot m^{-1} \cdot K^{-1}$ was due to the presence of macropores in the aerogels prepared by such a method. The team tested a spray freeze-drying technique in order to overcome the aforementioned issue. Aerogels showed a porous interconnected morphology with a pore size ranging from a few tenths of nanometers to a few microns. The lowest thermal conductivity reported was 0.018 $W \cdot m^{-1} \cdot K^{-1}$.

Coquard & Baillis [25] developed a numerical model for estimating the phonon thermal conductivity of cellulose-based aerogels in order to gain a deeper understanding of its thermal behavior. The model used a Kelvin cell representation of the porous structure whose size varied between 57 and 500 nm. At a fixed density, the aerogels with small cells reduced the phonon transport, and consequently, the heat flux due to interactions between phonons and the boundary of the solid phase.

Beyond 100 nm, phonon–phonon scattering events were predominant and the macroscopic laws of heat conduction were then applicable.

Jiménez-Saelices et al. [26] also prepared aerogels from freeze-dried cellulose-stabilized Pickering emulsions as gels (refer to Figure 3). It was claimed that the resistance of these emulsions to shrinkage during sublimation was responsible for the formation of an alveolar morphology and a closed porosity in the walls of such alveolar cells. The aerogels showed low thermal conductivities (0.018 $W \cdot m^{-1} \cdot K^{-1}$) in the "super-insulating" range.

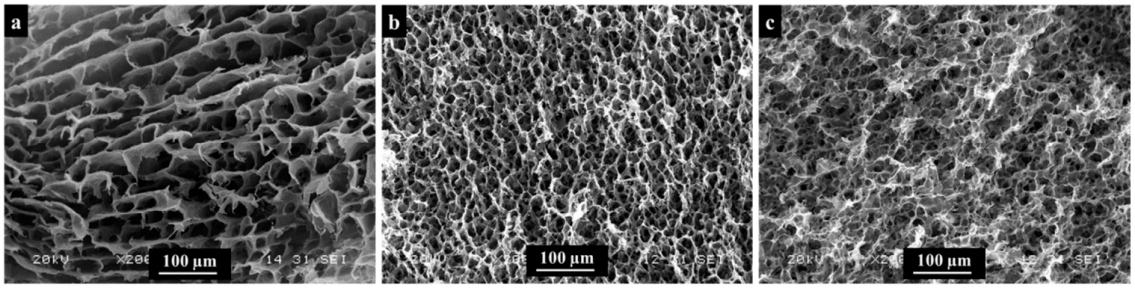

Figure 3. SEM images of aerogels prepared from cellulose-stabilized emulsions at different concentrations: (**a**) 1 wt %, (**b**) 2 wt %, and (**c**) 3 wt %. Reprinted with permission from [26]. Copyright 2018 American Chemical Society.

3. Challenges for Practical Application of Cellulose Aerogels in Thermal Insulation

In addition to thermal performance-related requirements strictly associated with the main function of thermal insulator materials, there are several challenges that need to be overcome for the practical application of cellulose aerogels for such a function.

3.1. Moisture Sensitivity

The hydrophilic characteristic of cellulose is detrimental for the thermal performance of the aerogels because it induces an eventual increase in thermal conductivity of the material through densification of the matrix as air moisture is retained. In a study carried out by Apostolopoulou-Kalkavoura et al. [27], the thermal conductivity of cellulose foams increased more than threefold as the relative humidity (RH) did from 2% to 80%. The main strategy aiming to solve the moisture sensitivity of cellulose involves modification of the surface of the aerogel.

Shi et al. [28,29] performed a hydrophobic modification of cellulose/silica aerogels using CCl_4 as plasma. The aerogels were prepared using NaOH/thiourea as a solvent system and the freeze-drying method. The modification turned the surface of aerogels from hydrophilic to hydrophobic, reporting a water contact angle of 132° for the cellulose/silica system.

Zhai et al. [30] formed poly(vinyl alcohol)/cellulose aerogels using a unidirectional freeze-drying process followed by chemical vapor deposition of methyltrichlorosilane. The silane-coated aerogels became hydrophobic, reporting a water contact angle of 141.8°.

Li et al. [31] fabricated cellulose/silica aerogels surface-treated by immersion in a trimethylchlorosilane/n-hexane solution. The aerogels reported a water contact angle of 139.6°. Trimethylchlorosilane reacts with water and Si–OH groups on the surface of the aerogels, substituting the hydrophilic –OH groups with hydrophobic $–CH_3$ groups.

Jiang et al. [32] aimed to simultaneously improve the mechanical properties and increase hydrophobicity of cellulose nanofibril aerogels by cross-linking cellulose at their surface hydroxyls with diisocyanate. Cross-linked aerogels reported a higher modulus (209 kPa) than their counterparts (94 kPa).

3.2. Flame-Retardant Performance and Thermal Stability

Cellulose by itself is a highly flammable biopolymer with a limiting oxygen index (LOI) near 18 [33]. Furthermore, the large surface area of cellulose aerogels facilitates the ignition process. LOI is a measure of the limiting concentration of oxygen in an oxygen/nitrogen mixture necessary for sustaining combustion once a material is ignited. Therefore, a material with an LOI value above 21 should not burn in air (at room temperature) unless there is a constant transfer of heat from a source. The general strategy explored to overcome this issue is to create cellulose-composite aerogels either by addition or in situ formation of flame-retardant agents. In this regard, inorganic nanoparticles are the main choice.

Fan et al. [34] prepared an aerogel based on cellulose nanofibrils and aluminum oxyhydroxide. Aluminum oxyhydroxide is a widely used inorganic flame-retardant additive because of its non-toxic and non-volatile nature. When exposed to a flame, the aerogel did not burn, and kept an integrated shape even after 60 s of continuous exposure. A control sample aerogel made only of cellulose nanofibrils burned immediately upon contact with the flame.

Yang et al. [35] prepared an aerogel consisting of a cellulose nanofibril backbone encapsulated by a layer of ultrathin MoS_2 nanosheets. The nanocomposite aerogel reported an LOI of 34.7 and a thermal conductivity of 0.028 $W \cdot m^{-1} \cdot K^{-1}$. A vertical burning test further demonstrated a self-extinguishing capability of the aerogel. Evidence suggested the presence of bonding between MoS_2 nanosheets and the cellulose nanofibril as a result of chemical cross-linking between Mo^{4+} cations, and carboxyl (–COOH) and hydroxyl (–OH) groups in the cellulose.

Han et al. [36] proposed an alternative approach to the conventional mixing of flame-retardant additives with cellulose nanofibrils, aiming to avoid additive agglomeration. The team used a three-dimensional nanoporous cellulose gel prepared by dissolution and coagulation of cellulose from an aqueous NaOH/urea solution as template for the growth of magnesium-hydroxide nanoparticles. Once ignited, the flame propagation slowed and extinguished within 40 s for the cellulose/MgOH aerogel. A control pure cellulose aerogel completely burned after 10 s.

Köklükaya et al. [37] deposited nanometric films of cationic chitosan, anionic poly(vinylphosphonic acid), and anionic montmorillonite clay on cellulose nanofibril aerogels through a layer-by-layer approach. The aerogels showed a non-ignition behavior when exposed to heat flux, whereas an unmodified sample ignited and burned completely. It was suggested that chitosan, poly(vinylphosphonic acid), and montmorillonite promote char formation and reduce the release of flammable volatiles.

Kaya [38] prepared a cellulose nanofibril aerogel cross-linked with citric acid. The non-cross-linked aerogel, once ignited, burned 25% of the sample after 34 s. The cross-linked aerogel was more slowly ignited and 25% of the sample burned after 51 s.

The thermal degradation of cellulose in nitrogen is a one-step process involving a competition between depolymerization and dehydration. In air, cellulose undergoes a two-step thermo-oxidation process: (i) aliphatic char and flammable volatile formation (at 300–400 °C) and (ii) oxidation of aliphatic char (at 400–600 °C) and release of carbon monoxide and dioxide [39]. Smith et al. [40] coated cellulose nanofibril aerogel with aluminum oxide through atomic layer deposition aiming toward improving the oxidation resistance of cellulose. The temperature of onset decomposition increased by 120 °C.

Silica layers were grown on the surface of bacterial cellulose nanofibrils in order to prepare freeze-dried aerogels by Liu et al. [41]. The silica-coated cellulose nanofibrils were further exposed to >400 °C, removing the cellulose cores and leading to silica nanotubes with internal dimensions equivalent to the dimensions of the nanofibrils. The decomposition temperature shifted 70 °C, reaching 335 °C under nitrogen atmosphere. The coverage of silica on the cellulose restricted the accessibility of oxygen and limited the degassing of degradation products.

Hydroxyapatite is an inorganic component found in bones making it an abundant and non-toxic choice as a flame-retardant additive. This motivated Guo et al. [42] to fabricate a series of cellulose/hydroxyapatite aerogels through a freeze-drying approach. Although the thermal

conductivity was relatively high (0.038 $W \cdot m^{-1} \cdot K^{-1}$), the addition of the inorganic phase provided the material a low peak heat release rate (20.4 $kW \cdot m^{-2}$) and total heat release (1.21 $MJ \cdot m^{-2}$) according to cone calorimetry tests. It was believed that the layer of hydroxyapatite covering cellulose nanofibers inhibited oxygen diffusion into the fibers, restricting the escape of volatile products.

3.3. Processing Energy Demand and Cost of Cellulose Aerogels

"Super-insulating" cellulose aerogels were reported promising half the material thickness for thermal insulation panels compared to expanded polystyrene, polyurethane, fiberglass, or mineral wool. However, the cost of an aerogel panel (silica for example) is up to 10 times that of those made of traditional insulation materials [43]. Although cellulose aerogels are only developed and tested at the lab scale so far, they are expected to have the same cost tendency as conventional aerogel panels. The cost of the panel is partially dictated by raw materials and their processing toward aerogel formation. In this regard, the main drawbacks of both supercritical-drying and freeze-drying approaches are their high capital investment, high energy demand, and long processing times.

In principle, breakthroughs in cost reduction of cellulose aerogel production could be achieved by performing the process at pressures and temperatures near atmospheric reference. Therefore, ambient pressure drying (APD) was proposed as a suitable alternative to FD and SD. For this approach to be effective, the collapse of the porous structure during drying due to capillary forces must be avoided. The general strategy to accomplish the aforementioned goal involves surface modification of cellulose into a hydrophobic nature. The techniques used to transform cellulose surfaces into a hydrophobic nature during APD differ from those presented in Section 3.1 because the former must be performed prior drying of the hydrogel. Surface modifications using trityl chloride [44], anhydride [45], and octylamine [46] were reported. In addition to surface hydrophobization, enhancing the hydrogel mechanical strength by means of cellulose nanofibril entanglement allowed the formation of low-density (0.018 $g \cdot cm^{-3}$) APD aerogels [47].

APD requires solvent exchange prior to drying; examples in the literature include the use of n-hexane [48], 2-propanol [47], ethanol [49,50], and 2-propanol followed by octane [51]. This represents another opportunity for cost reduction: finding ways to incorporate solvents with low vapor pressure, such as ionic liquids [52]. Upon finding a suitable ionic solvent for cellulose aerogel processing, the main advantage will be the opportunity to reuse these solvents after the drying step.

De France et al. [53] identified other processing methods that could reduce the cost of aerogel preparation by targeting scalability, including spray drying, freeze spray drying, and pressurized gas-expanded drying.

4. Cellulose/Silica Aerogels for Thermal Insulation

Silica aerogels are recognized due to their low thermal conductivity (–0.012 $W \cdot m^{-1} \cdot K^{-1}$) and low flammability [54]. Production costs and brittle mechanical behavior hinder their application for thermal insulation. To overcome this, several strategies were reported involving cellulose nanofibrils as cross-linkers or as a scaffold/template for aerogel formation. However, the improvement in mechanical properties generally comes at the expense of an increase in thermal conductivity of the resulting composite due to densification of the aerogel by the addition of a reinforcement phase. For example, Sai et al. [55] used a freeze-dried bacterial cellulose fibrous mat impregnated with silica-based sol to obtain a composite achieving a thermal conductivity of 0.037 $W \cdot m^{-1} \cdot K^{-1}$ compared to 0.030 $W \cdot m^{-1} \cdot K^{-1}$ for cellulose aerogel alone.

Zhao et al. [56] formed an interpenetrating network of mesoporous silica within a silylated-cellulose nanofibril template. The cellulose/silica system reported increases (relative to a control silica aerogel) in the Young modulus and ultimate stress under compression of 55% and 126%, respectively, while maintaining a thermal conductivity of 0.017 $W \cdot m^{-1} \cdot K^{-1}$.

Wong et al. [57] prepared a cellulose/silica aerogel by dispersing cellulose nanofibrils on a poly(ethoxydisiloxane) sols prior to gelation. No significant enhancements in elastic modulus,

compressive strength, or fracture strain could be identified or separated from the effects of increasing density. However, the cellulose/silica aerogel reported tensile strengths 25%–40% higher than that for a silica aerogel of comparable density. The thermal conductivity of the cellulose/silica system increased by −11% relative to the silica aerogel.

Silica aerogels are formed through a two-step acid–base-catalyzed sol–gel route from tetraalkoxysilane precursors. Therefore, Fu et al. [58] evaluated the effect of cellulose nanofibril concentration, tetraethyl orthosilicate concentration, pH of the condensation process, and immersion time on the physical and mechanical properties of cellulose/silica aerogels. Aerogels were prepared by the impregnation of a cellulose aerogel with a solution of silica, and subsequent hydrolysis and condensation at different pH values [59]. Optimal process parameters were determined through response surface methodology based on a Box–Behnken experimental design. The compressive Young modulus and the ultimate strength were 13–36 times higher and 8–30 times higher, respectively, when compared with silica aerogel.

Demilecamps et al. [60] aimed to decrease the thermal conductivity of cellulose/silica aerogels by "filling" their pores with silica and using cellulose as the backbone. The thermal conductivity decreased from 0.033 $W \cdot m^{-1} \cdot K^{-1}$ for an all-cellulose aerogel to 0.027 $W \cdot m^{-1} \cdot K^{-1}$ for the cellulose/silica system. The thermal conductivity remained above the "super-insulating" range possibly due to the increase in skeletal heat conduction of the composite with the increasing load on silica.

Laskowski et al. [61] approached a strategy to get cellulose/silica aerogel composites in which silica particles were added during the formation of a cellulose aerogel without disturbing the process of gel conformation. The thermal conductivity lay between 0.040 and 0.052 $W \cdot m^{-1} \cdot K^{-1}$ due to the fibrillary three-dimensional network continuously connected that allowed heat conduction through the backbone.

5. Outlook

Cellulose aerogels with "super-insulating" performance (thermal conductivity <0.025 $W \cdot m^{-1} \cdot K^{-1}$) can be produced through supercritical-drying or freeze-drying. However, the nature of such processes lags the commercialization of the aerogels. The main reasons associated with the aforementioned issue involves challenges in the industrial scalability of the processes, the slow-batch nature of the methods, and the need for specialized equipment due to the temperatures and pressures required. Furthermore, these processes are intensive in chemical usage (*N*-methylmorpholine *N*-oxide, alkali hydroxide/urea, lithium chloride/dimethylacetamine, and lithium chloride/dimethyl sulfoxide to name a few [62]) imparting questions about their sustainability. Therefore, there is a need for novel sustainable cost-effective processes like APD. In addition to APD, other techniques were also reported, although they were either less or not explored for thermal insulation, such as vacuum filtration [51] and freeze-casting [63]. Other techniques used for porous scaffold synthesis for tissue engineering could be explored in order to assess their feasibility in the fabrication of cellulose aerogels, including electrospinning [64], additive manufacturing [65], gas-foaming [66], and compression-molding [67], among others.

Cellulose by itself is an attractive choice as a raw material for aerogel construction because of its natural abundance. However, cellulose nanofibrils, with a diameter of 5–20 nm, constitute the backbone of reported aerogels. These nanofibrils are not widely commercially available because their production is time-consuming and their yield is usually low [68]. Furthermore, depending on the cellulose source and isolation technique, the resulting nanofibril can vary in crystal structure, degree of crystallinity, morphology, aspect ratio, and surface chemistry [69]. Despite the concern, no detailed studies could be found regarding the effect of these parameters on aerogel thermal performance.

Table 2 is a summary of the properties of cellulose aerogels reported within the last five years. Direct comparison among aerogel properties is interfered with by the lack of standardized characterization protocols. Furthermore, most studies focus on the characteristics of the aerogels themselves. Inspection of Table 2 suggests that SD offers lower thermal conductivities than FD.

This could be explained because the growth of ice crystals during FD leads to larger pores compared to SD. A minimum in thermal conductivity is reached for a specific aerogel density. This is because the contribution of solid-phase heat conduction increases with density, whereas, at really low densities, pore size goes beyond 70 nm.

Table 2. Properties of interest for selected cellulose aerogels gathered from scientific articles published within the last five years.

Material	Aerogel Formation Method	Density ($g \cdot cm^{-3}$)	Young Modulus (MPa)	Ultimate Strength (MPa)	Thermal Conductivity ($W \cdot m^{-1} \cdot K^{-1}$)	T_{Onset} (°C)	Water Contact Angle (°)	LOI (%)
Cellulose (HCl hydrolysis) [17]	FD	0.005	–	–	0.016	342	–	–
Cellulose (surface-carboxylated) [18]	SD	0.017	0.40	–	0.018	–	–	–
Cellulose [18]	–	–	–	13.000	0.030	–	–	–
Cellulose (TEMPO-mediated oxidation) [22]	FD	–	0.10	–	0.018	–	–	–
Cellulose (TEMPO-mediated oxidation) [9]	FD	–	–	–	0.022	–	–	–
	SD	–	–	–	0.017	–	–	–
Cellulose (TEMPO-mediated oxidation) [23]	FD	0.035	0.18	–	0.023	–	–	–
Cellulose (TEMPO-mediated oxidation) [24]	Spray FD	0.022	–	–	0.018	–	–	–
Cellulose (TEMPO-mediated oxidation) [20]	FD	0.020	–	–	0.024	–	–	–
Cellulose/silica + cold plasma modification [28,29]	FD	0.023	–	–	0.026	–	132.0	–
Cellulose [26]	FD	0.020	0.60	–	0.018	–	–	–
Poly(vinyl alcohol)/ cellulose (TEMPO-mediated oxidation) + chemical vapor deposition of methyltrichlorosilane [30]	Unidirectional FD	0.018	10.4	–	–	495 at N_2	141.8	–
Cellulose(sulfuric acid hydrolysis)/silica [31]	APD	0.137	–	–	0.035	253 at air	139.6	–
Cellulose cross-linked with diisocyanate [32]	Freezing–thawing	–	0.209	0.066	–	200 at N_2	–	–
Cellulose/MoS_2 [35]	FD	0.005	0.326	–	0.028	300 at air	–	34.7
Cellulose/MgOH [36]	FD	0.400	–	0.467	0.081	225 at N_2	–	–
Cellulose/poly(vinyl alcohol)/chitosan/ montmorillonite [37]	FD	–	–	–	–	273 at air	–	–
Cellulose/aluminum oxide [40]	SD	–	–	–	–	295 at air	–	–
Bacterial cellulose/silica [41]	FD	–	–	–	–	335 at N_2	–	–
Cellulose/silica [56]	SD	0.122	1.750	0.375	0.017	–	–	–
Cellulose/silica [57]	SD	0.143	2.200	1.500	0.015	–	-	–
Cellulose/silica [58]	APD	0.100	6.570	1.37	0.023	–	152.1	–
Cellulose/silica [60]	SD	0.225	11.500	–	0.027	–	–	–
Cellulose/silica [61]	SD	0.150	2.000	–	0.045	–	–	–
Cellulose/hydroxipatite [42]	FD	–	0.253	0.060	0.038	–	–	–

FD: freeze-drying; SD: supercritical-drying; APD: ambient pressure drying; T_{Onset}: initial decomposition temperature; LOI: limiting oxygen index; TEMPO: (2,2,6,6-tetramethylpiperidin-1-yl)oxidanyl.

Regarding the composite-based strategies for overcoming moisture sensitivity, flammability, and thermal stability, the main challenge is associated with the solution-based approach for composite-cellulose aerogel formation. In particular, the question to be answered is how to get a fine dispersion of the cellulose/host component into the viscous cellulose hydrogel without disrupting the distribution of the dispersed solids during solvent removal. Similarly, the improvement in mechanical properties of silica/cellulose aerogels comes at the expense of high loading of cellulose in the system. However, increasing the cellulose content may lead to an increase in density and a subsequent decrease in pore size, which will negatively impact thermal insulation performance.

6. Conclusions

Cellulose-based aerogels can have thermal conductivities as low as –0.015 $W \cdot m^{-1} \cdot K^{-1}$ falling into the category of "super-insulating" materials. This range of thermal conductivities seems to be a consequence of an interplay between different factors, such as a non-interconnected porous morphology with an average pore size bellow 70 nm. Low density (<0.025 $g \cdot cm^{-3}$) is also required to decrease the contribution of heat conduction through the solid matrix. However, a continuous decrease in density will eventually lead to an increase in pore size beyond 70 nm, thereby increasing the thermal conduction of the porous solid.

The following topics could be drawn as points of interest for further development of cellulose aerogels as thermal insulators in buildings:

- In addition to cost reduction, the improvement of cellulose aerogel production techniques should also point toward sustainability. Otherwise, the benefits from cellulose as a raw material will be swept away by processing.
- Improvements in moisture sensitivity, flammability, and thermal stability of aerogels following the current approaches will come at the expense of a densification of the porous matrix, increasing the contribution of solid conduction.
- The effects of crystal structure, degree of crystallinity, morphology, aspect ratio, and surface chemistry of cellulose nanofibrils on the cellulose aerogel thermal performance are partially understood.
- Defining and adopting standardized aerogel characterization protocols is required to allow proper comparison among research outcomes. In particular, for the determination of thermal conductivity, the guarded hot-plate technique is considered the most accurate and reliable for such a matter, although other techniques such as transient hot-wire/hot disk and laser flash analysis represent suitable alternatives.

Author Contributions: Conceptualization, D.I.; Investigation, D.I. and J.M.; Resources, D.I. and J.M.; Writing-Original Draft Preparation, D.I. and J.M.; Writing-Review & Editing, D.I., J.M., H.M. and H.G.; Supervision, H.M. and H.G.; Project Administration, H.M. and H.G.

Acknowledgments: The authors would like to acknowledge the Universidad Del Norte and the Departamento Administrativo de Ciencia, Tecnología e Innovación (Colciencias) for the support given within the framework of the PhD National Scholarship Colciencias N° 617-2014 (Contract Identification Number UN-OJ-2014-26159 and UN-OJ-2014-24072).

Conflicts of Interest: The authors declare no conflicts of interest. The founding sponsors had no role in the design of the study; in the collection, analyses, or interpretation of data; in the writing of the manuscript, and in the decision to publish the results.

References

1. LaFrance, M. *Technology Roadmap: Energy Efficient Building Envelopes*; IEA: Paris, France, 2013.
2. Mirrahimi, S.; Mohamed, M.F.; Haw, L.C.; Ibrahim, N.L.N.; Yusoff, W.F.M.; Aflaki, A. The effect of building envelope on the thermal comfort and energy saving for high-rise buildings in hot–humid climate. *Renew. Sustain. Energy Rev.* **2016**, *53*, 1508–1519. [CrossRef]
3. Asdrubali, F.; D'Alessandro, F.; Schiavoni, S. A review of unconventional sustainable building insulation materials. *Sustain. Mater. Technol.* **2015**, *4*, 1–17. [CrossRef]
4. Jelle, B.P. Traditional, state-of-the-art and future thermal building insulation materials and solutions—Properties, requirements and possibilities. *Energy Build.* **2011**, *43*, 2549–2563. [CrossRef]
5. Moon, R.J.; Martini, A.; Nairn, J.; Simonsen, J.; Youngblood, J. Cellulose nanomaterials review: Structure, properties and nanocomposites. *Chem. Soc. Rev.* **2011**, *40*, 3941–3994. [CrossRef] [PubMed]
6. Long, L.-Y.; Weng, Y.-X.; Wang, Y.-Z. Cellulose Aerogels: Synthesis, Applications, and Prospects. *Polymers* **2018**, *10*, 623. [CrossRef]
7. Nič, M.; Jirát, J.; Košata, B.; Jenkins, A.; McNaught, A. *IUPAC Compendium of Chemical Terminology*, 2nd ed.; IUPAC: Research Triagle Park, NC, USA, 2009.

8. Pierre, A.C. History of Aerogels. In *Aerogels Handbook*; Aegerter, M.A., Leventis, N., Koebel, M.M., Eds.; Springer: New York, NY, USA, 2011; pp. 3–18.
9. Sakai, K.; Kobayashi, Y.; Saito, T.; Isogai, A. Partitioned airs at microscale and nanoscale: Thermal diffusivity in ultrahigh porosity solids of nanocellulose. *Sci. Rep.* **2016**, *6*, 20434. [CrossRef] [PubMed]
10. Lavoine, N.; Bergström, L. Nanocellulose-based foams and aerogels: Processing, properties, and applications. *J. Mater. Chem. A* **2017**, *5*, 16105–16117. [CrossRef]
11. Şahin, İ.; Özbakır, Y.; İnönü, Z.; Ulker, Z.; Erkey, C. Kinetics of Supercritical Drying of Gels. *Gels* **2017**, *4*, 3. [CrossRef]
12. García-González, C.A.; Camino-Rey, M.C.; Alnaief, M.; Zetzl, C.; Smirnova, I. Supercritical drying of aerogels using CO_2: Effect of extraction time on the end material textural properties. *J. Supercrit. Fluids* **2012**, *66*, 297–306. [CrossRef]
13. Fricke, J. Thermal transport in porous superinsulations. In *Aerogels*; Springer: New York, NY, USA, 1986; pp. 94–103.
14. Fricke, J.; Emmerling, A. Aerogels. *J. Am. Ceram. Soc.* **1992**, *75*, 2027–2035. [CrossRef]
15. Vargaftik, N.B. *Handbook of Thermal Conductivity of Liquids and Gases*; CRC Press: Boca Raton, FL, USA, 1993.
16. Smith, D.M.; Maskara, A.; Boes, U. Aerogel-based thermal insulation. *J. Non-Cryst. Solids* **1998**, *225*, 254–259. [CrossRef]
17. Chen, W.; Li, Q.; Wang, Y.; Yi, X.; Zeng, J.; Yu, H.; Liu, Y.; Li, J. Comparative Study of Aerogels Obtained from Differently Prepared Nanocellulose Fibers. *ChemSusChem* **2014**, *7*, 154–161. [CrossRef] [PubMed]
18. Buesch, C.; Smith, S.W.; Eschbach, P.; Conley, J.F.; Simonsen, J. The Microstructure of Cellulose Nanocrystal Aerogels as Revealed by Transmission Electron Microscope Tomography. *Biomacromolecules* **2016**, *17*, 2956–2962. [CrossRef] [PubMed]
19. Kobayashi, Y.; Saito, T.; Isogai, A. Aerogels with 3D Ordered Nanofiber Skeletons of Liquid-Crystalline Nanocellulose Derivatives as Tough and Transparent Insulators. *Angew. Chem. Int. Ed.* **2014**, *53*, 10394–10397. [CrossRef] [PubMed]
20. Jiménez-Saelices, C.; Seantier, B.; Cathala, B.; Grohens, Y. Effect of freeze-drying parameters on the microstructure and thermal insulating properties of nanofibrillated cellulose aerogels. *J. Sol-Gel Sci. Technol.* **2017**, *84*, 475–485. [CrossRef]
21. Li, T.; Song, J.; Zhao, X.; Yang, Z.; Pastel, G.; Xu, S.; Jia, C.; Dai, J.; Chen, C.; Gong, A.; et al. Anisotropic, lightweight, strong, and super thermally insulating nanowood with naturally aligned nanocellulose. *Sci. Adv.* **2018**, *4*, eaar3724. [CrossRef] [PubMed]
22. Bendahou, D.; Bendahou, A.; Seantier, B.; Grohens, Y.; Kaddami, H. Nano-fibrillated cellulose-zeolites based new hybrid composites aerogels with super thermal insulating properties. *Ind. Crops Prod.* **2015**, *65*, 374–382. [CrossRef]
23. Seantier, B.; Bendahou, D.; Bendahou, A.; Grohens, Y.; Kaddami, H. Multi-scale cellulose based new bio-aerogel composites with thermal super-insulating and tunable mechanical properties. *Carbohydr. Polym.* **2016**, *138*, 335–348. [CrossRef] [PubMed]
24. Jiménez-Saelices, C.; Seantier, B.; Cathala, B.; Grohens, Y. Spray freeze-dried nanofibrillated cellulose aerogels with thermal superinsulating properties. *Carbohydr. Polym.* **2017**, *157*, 105–113. [CrossRef] [PubMed]
25. Coquard, R.; Baillis, D. Thermal conductivity of Kelvin cell cellulosic aerogels: Analytical and Monte Carlo approaches. *J. Mater. Sci.* **2017**, *52*, 11135–11145. [CrossRef]
26. Jiménez-Saelices, C.; Seantier, B.; Grohens, Y.; Capron, I. Thermal Superinsulating Materials Made from Nanofibrillated Cellulose-Stabilized Pickering Emulsions. *ACS Appl. Mater. Interfaces* **2018**, *10*, 16193–16202. [CrossRef] [PubMed]
27. Apostolopoulou-Kalkavoura, V.; Gordeyeva, K.; Lavoine, N.; Bergström, L. Thermal conductivity of hygroscopic foams based on cellulose nanofibrils and a nonionic polyoxamer. *Cellulose* **2018**, *25*, 1117–1126. [CrossRef]
28. Shi, J.; Lu, L.; Guo, W.; Sun, Y.; Cao, Y. An environment-friendly thermal insulation material from cellulose and plasma modification. *J. Appl. Polym. Sci.* **2013**, *130*, 3652–3658. [CrossRef]
29. Shi, J.; Lu, L.; Guo, W.; Zhang, J.; Cao, Y. Heat insulation performance, mechanics and hydrophobic modification of cellulose–SiO_2 composite aerogels. *Carbohydr. Polym.* **2013**, *98*, 282–289. [CrossRef] [PubMed]

30. Zhai, T.; Zheng, Q.; Cai, Z.; Turng, L.-S.; Xia, H.; Gong, S. Poly(vinyl alcohol)/Cellulose Nanofibril Hybrid Aerogels with an Aligned Microtubular Porous Structure and Their Composites with Polydimethylsiloxane. *ACS Appl. Mater. Interfaces* **2015**, *7*, 7436–7444. [CrossRef] [PubMed]
31. Li, M.; Jiang, H.; Xu, D.; Yang, Y. A facile method to prepare cellulose whiskers–silica aerogel composites. *J. Sol-Gel Sci. Technol.* **2017**, *83*, 72–80. [CrossRef]
32. Jiang, F.; Hsieh, Y.-L. Cellulose Nanofibril Aerogels: Synergistic Improvement of Hydrophobicity, Strength, and Thermal Stability via Cross-Linking with Diisocyanate. *ACS Appl. Mater. Interfaces* **2017**, *9*, 2825–2834. [CrossRef] [PubMed]
33. Tian, C.M.; Shi, Z.H.; Zhang, H.Y.; Xu, J.Z.; Shi, J.R.; Guo, H.Z. Thermal degradation of cotton cellulose. *J. Therm. Anal. Calorim.* **1999**, *55*, 93–98. [CrossRef]
34. Fan, B.; Chen, S.; Yao, Q.; Sun, Q.; Jin, C. Fabrication of cellulose nanofiber/AlOOH aerogel for flame retardant and thermal insulation. *Materials* **2017**, *10*, 311. [CrossRef] [PubMed]
35. Yang, L.; Mukhopadhyay, A.; Jiao, Y.; Yong, Q.; Chen, L.; Xing, Y.; Hamel, J.; Zhu, H. Ultralight, highly thermally insulating and fire resistant aerogel by encapsulating cellulose nanofibers with two-dimensional MoS_2. *Nanoscale* **2017**, *9*, 11452–11462. [CrossRef] [PubMed]
36. Han, Y.; Zhang, X.; Wu, X.; Lu, C. Flame Retardant, Heat Insulating Cellulose Aerogels from Waste Cotton Fabrics by in Situ Formation of Magnesium Hydroxide Nanoparticles in Cellulose Gel Nanostructures. *ACS Sustain. Chem. Eng.* **2015**, *3*, 1853–1859. [CrossRef]
37. Köklükaya, O.; Carosio, F.; Wågberg, L. Superior Flame-Resistant Cellulose Nanofibril Aerogels Modified with Hybrid Layer-by-Layer Coatings. *ACS Appl. Mater. Interfaces* **2017**, *9*, 29082–29092. [CrossRef] [PubMed]
38. Kaya, M. Super absorbent, light, and highly flame retardant cellulose-based aerogel crosslinked with citric acid. *J. Appl. Polym. Sci.* **2017**, *134*, 45315. [CrossRef]
39. Soares, S.; Camino, G.; Levchik, S. Comparative study of the thermal decomposition of pure cellulose and pulp paper. *Polym. Degrad. Stab.* **1995**, *49*, 275–283. [CrossRef]
40. Smith, S.W.; Buesch, C.; Matthews, D.J.; Simonsen, J.; Conley, J.F. Improved oxidation resistance of organic/inorganic composite atomic layer deposition coated cellulose nanocrystal aerogels. *J. Vac. Sci. Technol. A Vac. Surf. Film.* **2014**, *32*, 041508. [CrossRef]
41. Liu, D.; Wu, Q.; Andersson, R.L.; Hedenqvist, M.S.; Farris, S.; Olsson, R.T. Cellulose nanofibril core–shell silica coatings and their conversion into thermally stable nanotube aerogels. *J. Mater. Chem. A* **2015**, *3*, 15745–15754. [CrossRef]
42. Guo, W.; Wang, X.; Zhang, P.; Liu, J.; Song, L.; Hu, Y. Nano-fibrillated cellulose-hydroxyapatite based composite foams with excellent fire resistance. *Carbohydr. Polym.* **2018**, *195*, 71–78. [CrossRef] [PubMed]
43. Koebel, M.; Rigacci, A.; Achard, P. Aerogel-based thermal superinsulation: An overview. *J. Sol-Gel Sci. Technol.* **2012**, *63*, 315–339. [CrossRef]
44. Pour, G.; Beauger, C.; Rigacci, A.; Budtova, T. Xerocellulose: Lightweight, porous and hydrophobic cellulose prepared via ambient drying. *J. Mater. Sci.* **2015**, *50*, 4526–4535. [CrossRef]
45. Sehaqui, H.; Zimmermann, T.; Tingaut, P. Hydrophobic cellulose nanopaper through a mild esterification procedure. *Cellulose* **2014**, *21*, 367–382. [CrossRef]
46. Cervin, N.T.; Andersson, L.; Ng, J.B.S.; Olin, P.; Bergström, L.; Wågberg, L. Lightweight and Strong Cellulose Materials Made from Aqueous Foams Stabilized by Nanofibrillated Cellulose. *Biomacromolecules* **2013**, *14*, 503–511. [CrossRef] [PubMed]
47. Li, Y.; Tanna, V.A.; Zhou, Y.; Winter, H.H.; Watkins, J.J.; Carter, K.R. Nanocellulose Aerogels Inspired by Frozen Tofu. *ACS Sustain. Chem. Eng.* **2017**, *5*, 6387–6391. [CrossRef]
48. Fu, J.; He, C.; Wang, S.; Chen, Y. A thermally stable and hydrophobic composite aerogel made from cellulose nanofibril aerogel impregnated with silica particles. *J. Mater. Sci.* **2018**, *53*, 7072–7082. [CrossRef]
49. Zhang, X.; Liu, P.; Duan, Y.; Jiang, M.; Zhang, J. Graphene/cellulose nanocrystals hybrid aerogel with tunable mechanical strength and hydrophilicity fabricated by ambient pressure drying technique. *RSC Adv.* **2017**, *7*, 16467–16473. [CrossRef]
50. Markevicius, G.; Ladj, R.; Niemeyer, P.; Budtova, T.; Rigacci, A. Ambient-dried thermal superinsulating monolithic silica-based aerogels with short cellulosic fibers. *J. Mater. Sci.* **2017**, *52*, 2210–2221. [CrossRef]
51. Toivonen, M.S.; Kaskela, A.; Rojas, O.J.; Kauppinen, E.I.; Ikkala, O. Ambient-Dried Cellulose Nanofibril Aerogel Membranes with High Tensile Strength and Their Use for Aerosol Collection and Templates for Transparent, Flexible Devices. *Adv. Funct. Mater.* **2015**, *25*, 6618–6626. [CrossRef]

52. Shukla, N.; Fallahi, A.; Kosny, J. Aerogel Thermal Insulation-Technology Review and Cost Study for Building Enclosure Applications. *ASHRAE Trans.* **2014**, *120*, 294–307.
53. De France, K.J.; Hoare, T.; Cranston, E.D. Review of Hydrogels and Aerogels Containing Nanocellulose. *Chem. Mater.* **2017**, *29*, 4609–4631. [CrossRef]
54. Pierre, A.C.; Rigacci, A. SiO_2 Aerogels. In *Aerogels Handbook*; Springer: New York, NY, USA, 2011; pp. 21–45.
55. Sai, H.; Xing, L.; Xiang, J.; Cui, L.; Jiao, J.; Zhao, C.; Li, Z.; Li, F.; Zhang, T. Flexible aerogels with interpenetrating network structure of bacterial cellulose–silica composite from sodium silicate precursor via freeze drying process. *RSC Adv.* **2014**, *4*, 30453. [CrossRef]
56. Zhao, S.; Zhang, Z.; Sèbe, G.; Wu, R.; Rivera Virtudazo, R.V.; Tingaut, P.; Koebel, M.M. Multiscale assembly of superinsulating silica aerogels within silylated nanocellulosic scaffolds: Improved mechanical properties promoted by nanoscale chemical compatibilization. *Adv. Funct. Mater.* **2015**, *25*, 2326–2334. [CrossRef]
57. Wong, J.C.H.; Kaymak, H.; Tingaut, P.; Brunner, S.; Koebel, M.M. Mechanical and thermal properties of nanofibrillated cellulose reinforced silica aerogel composites. *Microporous Mesoporous Mater.* **2015**, *217*, 150–158. [CrossRef]
58. Fu, J.; He, C.; Huang, J.; Chen, Z.; Wang, S. Cellulose nanofibril reinforced silica aerogels: Optimization of the preparation process evaluated by a response surface methodology. *RSC Adv.* **2016**, *6*, 100326–100333. [CrossRef]
59. Fu, J.; Wang, S.; He, C.; Lu, Z.; Huang, J.; Chen, Z. Facilitated fabrication of high strength silica aerogels using cellulose nanofibrils as scaffold. *Carbohydr. Polym.* **2016**, *147*, 89–96. [CrossRef] [PubMed]
60. Demilecamps, A.; Beauger, C.; Hildenbrand, C.; Rigacci, A.; Budtova, T. Cellulose–silica aerogels. *Carbohydr. Polym.* **2015**, *122*, 293–300. [CrossRef] [PubMed]
61. Laskowski, J.; Milow, B.; Ratke, L. The effect of embedding highly insulating granular aerogel in cellulosic aerogel. *J. Supercrit. Fluids* **2015**, *106*, 93–99. [CrossRef]
62. Shen, X.; Shamshina, J.L.; Berton, P.; Gurau, G.; Rogers, R.D. Hydrogels based on cellulose and chitin: Fabrication, properties, and applications. *Green Chem.* **2016**, *18*, 53–75. [CrossRef]
63. Munier, P.; Gordeyeva, K.; Bergström, L.; Fall, A.B. Directional Freezing of Nanocellulose Dispersions Aligns the Rod-Like Particles and Produces Low-Density and Robust Particle Networks. *Biomacromolecules* **2016**, *17*, 1875–1881. [CrossRef] [PubMed]
64. Peng, F.; Shaw, M.T.; Olson, J.R.; Wei, M. Hydroxyapatite Needle-Shaped Particles/Poly(l-lactic acid) Electrospun Scaffolds with Perfect Particle-along-Nanofiber Orientation and Significantly Enhanced Mechanical Properties. *J. Phys. Chem. C* **2011**, *115*, 15743–15751. [CrossRef]
65. Yun, H.; Kim, S.; Hyun, Y.; Heo, S.; Shin, J. Three-Dimensional Mesoporous−Giantporous Inorganic/Organic Composite Scaffolds for Tissue Engineering. *Chem. Mater.* **2007**, *19*, 6363–6366. [CrossRef]
66. Chen, W.; Zhou, H.; Tang, M.; Weir, M.D.; Bao, C.; Xu, H.H.K. Gas-Foaming Calcium Phosphate Cement Scaffold Encapsulating Human Umbilical Cord Stem Cells. *Tissue Eng. Part A* **2012**, *18*, 816–827. [CrossRef] [PubMed]
67. Jing, D.; Wu, L.; Ding, J. Solvent-Assisted Room-Temperature Compression Molding Approach to Fabricate Porous Scaffolds for Tissue Engineering. *Macromol. Biosci.* **2006**, *6*, 747–757. [CrossRef] [PubMed]
68. Brinchi, L.; Cotana, F.; Fortunati, E.; Kenny, J.M. Production of nanocrystalline cellulose from lignocellulosic biomass: Technology and applications. *Carbohydr. Polym.* **2013**, *94*, 154–169. [CrossRef] [PubMed]
69. Sacui, I.A.; Nieuwendaal, R.C.; Burnett, D.J.; Stranick, S.J.; Jorfi, M.; Weder, C.; Foster, E.J.; Olsson, R.T.; Gilman, J.W. Comparison of the Properties of Cellulose Nanocrystals and Cellulose Nanofibrils Isolated from Bacteria, Tunicate, and Wood Processed Using Acid, Enzymatic, Mechanical, and Oxidative Methods. *ACS Appl. Mater. Interfaces* **2014**, *6*, 6127–6138. [CrossRef] [PubMed]